RESEARCH ARTICLE

National Science Open
3: 20230069, 2024
https://doi.org/10.1360/nso/20230069

Physics

Special Topic: Active Matter

Effective diffusion of a tracer in active bath: A path-integral approach

Mengkai Feng* & Zhonghuai Hou*

Hefei National Research Center for Physical Sciences at the Microscale & Key Laboratory of Precision and Intelligent Chemistry, University of Science and Technology of China, Hefei 230026, China

*Corresponding authors (emails: fengmk@ustc.edu.cn (Mengkai Feng); hzhlj@ustc.edu.cn (Zhonghuai Hou))

Received 30 October 2023; Revised 3 January 2024; Accepted 5 February 2024; Published online 1 April 2024

Abstract: We investigate the effective diffusion of a tracer immersed in an active particle bath consisting of self-propelled particles. Utilising the Dean's method developed for the equilibrium bath and extending it to the nonequilibrium situation, we derive a generalized Langevin equation (GLE) for the tracer particle. The complex interactions between the tracer and bath particles are shown as a memory kernel term and two colored noise terms. To obtain the effective diffusivity of the tracer, we use path integral technique to calculate all necessary correlation functions. Calculations show the effective diffusion decreases with the persistent time of active force, and has rich behavior with the number density of bath particles, depending on different activities. All theoretical results regarding the dependence of such diffusivity on bath parameters have been confirmed by direct computer simulation.

Keywords: active matter, nonequilibrium statistical mechanics, active bath, mean-field theory, path integral, tracer diffusivity

INTRODUCTION

Active matter systems, consisting of self-propelled units that are able to convert stored or surrounding energy into their persistent motion, provide a fresh opportunity for applications of nonequilibrium statistical mechanics [1–4]. In particular, active colloidal suspension can serve as an active bath that can significantly influence the motion and dynamics of passive objects submerged within them [5–12]. Understanding the behavior of tracer particles in the active bath is a fundamental pursuit in statistical physics and plays a crucial role in various biological [10, 13–16], chemical [17, 18], and physical phenomena [8, 9, 12, 19–32]. Notably, the tracer particle immersed in the active bath exhibits a distinct diffusion profile compared to its equilibrium counterpart [26, 33–39]. Furthermore, studying the diffusion behavior of such a tracer is essential for unraveling the intricate dynamics that govern systems away from thermal equilibrium, providing a valuable tool to investigate the collective behavior [8, 40–46] and transport properties in such media [47–51]. Because of the importance and wide range of applications, understanding the dynamics of the tracer in such an active bath is desirable.

As one already knows, the classical work by Einstein laid the foundation for understanding Brownian motion, providing a framework for diffusive behavior in passive media. Subsequent advancements, such as the Langevin equation, have enriched our understanding of stochastic processes, diffusive phenomena, and the fluctuation-dissipation theorem in thermal equilibrium. Nevertheless, the dynamics of particles in active baths introduce additional complexity [37,45,51–57]. Several studies have investigated this question, often employing analytical and numerical techniques to model and characterize the motion of tracer particles within nonequilibrium media, including the active bath. For instance, Maes *et al.* established a generalized fluctuation-response relation for thermal systems driven out of equilibrium [58–63], utilized this method to investigate the fluctuation-dissipation relation for nonequilibrium bath [35], and further studied the dynamics of a tracer immersed in such bath, gave the friction and noise properties [53], the Langevin description [64], and correlation functions of the tracer variables to study the fluctuation properties [54]. Speck and Seifert *et al.* formulated a fluctuation-dissipation theorem (FDT) within a nonequilibrium steady state of a sheared colloidal suspension system [65,66], and subsequently investigated the mobility and diffusivity of a tagged particle within this system, determined the velocity autocorrelation functions and response functions with small shear force, found that a phenomenological effective temperature recovers the Einstein relation in nonequilibrium [67]. Esparza-López *et al.* [68] proposed a stochastic fluid dynamic model to describe analytically and computationally the dynamics of microscopic particles driven by the motion of surface attached bacteria, analytically calculated expressions for the effective diffusion coefficient through a run-and-tumble model, found that the short-time mean squared displacement is proportional to the square of the swimming speed while the long-time one only depends on the size of the particle. Burkholder and Brady [22] studied the diffusion of a tracer in a dilute dispersion of active Brownian particles (ABPs), by employing the Smoluchowski equation and averaging over bath particles and orientation variables, obtained tracers single-particle probability distribution function, found that the active contribution to the diffusivity scales as U_0 (characteristic swim speed of ABP) for strong swimming and U_0^2 for weak swimming. Furthermore, they [69] derived a general relationship between diffusivity and mobility in generic colloidal suspensions, provided a method to quantify deviations from the FDT and express them in terms of an effective SES relation. More recently, Granek *et al.* [51] studied the long-time dynamics of a tracer immersed in a one-dimensional active bath, derived a time-dependent friction and noise correlation with power law long tails that depend on the symmetry of tracers, and found that shape asymmetry of the tracer induces ratchet effects and leads to super-diffusion and friction that grows with time.

Numerous theories based on various starting points have demonstrated the importance and attraction of studying tracer behavior in nonequilibrium baths. In this study, we propose an alternative theoretical method based on path-integral method to investigate the behavior of tracer diffusion in an active particle bath, and subsequent simulation results successfully validate our theory. The starting point of the theory is the generalized Langevin equation (GLE) for the tracer, which utilizes a generalized version of Dean's equation to describe the active bath. The GLE contains a memory kernel function and complex effective noise terms, reflecting the complex interactions between the tracer and bath particles. We then employ the path integral method [70,71] to calculate the diffusion coefficient. Numerical calculations show that the effective diffusion has a non-trivial dependence on bath parameters such as the number density and the persistent time of the active bath particle. Finally, we perform extensive computer simulations, which show very good agreement with our theoretical predictions.

This work is organized as follows: In Section "Model and theory" , we introduce the model system and derive the GLE of the tracer. Then, we utilize the path integral method to obtain the effective diffusion of

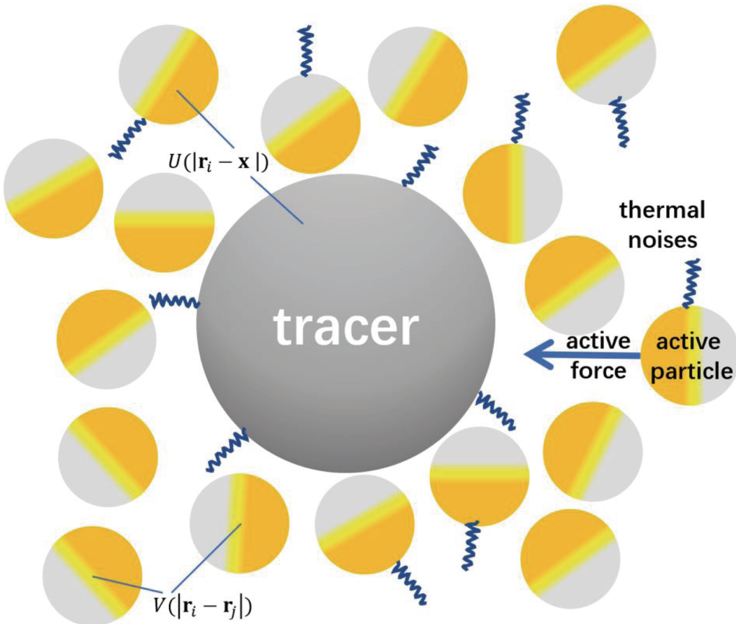

Figure 1 Schematic diagram of a tracer particle with coordinate $\mathbf{x}$ in an active particle bath consisting of self-propulsion particles at $\mathbf{r}_i$, $i = 1, 2, ..., N$. The tracer-bath interaction is $U(|\mathbf{x} - \mathbf{r}_i|)$, and the bath-bath interaction is $V(|\mathbf{r}_i - \mathbf{r}_j|)$. The wave lines label the thermal noises.

the tracer formally. In Section “Simulation results”, we show the numerical solution of such diffusion and compare it with simulation results. The paper ends with conclusion in Section “Conclusion”.

MODEL AND THEORY

Active bath model

Considering a system consisting of a tracer particle and N active Ornstein-Uhlenbeck (OU) particles (Figure 1), the coordinates of the tracer $\mathbf{x}$ and the active bath particles $\mathbf{r}_i$ are governed by the overdamped Langevin equations,

$$\dot{\mathbf{x}} = -\mu_t \nabla_x \left[\sum_{i=1}^{N} U(|\mathbf{x} - \mathbf{r}_i|) + U_{\text{ext}}(\mathbf{x}) \right] + \sqrt{2\mu_t T}\boldsymbol{\xi}_t, \tag{1a}$$

$$\dot{\mathbf{r}}_i = -\mu_b \left\{ \mathbf{f}_i + \nabla_i \left[\sum_{j \neq i} V(|\mathbf{r}_i - \mathbf{r}_j|) + U(|\mathbf{r}_i - \mathbf{x}|) \right] \right\} + \sqrt{2\mu_b T}\boldsymbol{\xi}_i, \tag{1b}$$

$$\tau_b \dot{\mathbf{f}}_i = -\mathbf{f}_i + \sqrt{2D_b/\mu_b^2}\boldsymbol{\eta}_i, \tag{1c}$$

wherein μ_t and μ_b are the mobilities of the tracer and bath particles respectively, U_{ext} is an external potential acting on the tracer particle, U is the interacting potential between tracer and bath particles, and V is potential between bath particles, $\boldsymbol{\xi}_t$, $\boldsymbol{\xi}_i$ and $\boldsymbol{\eta}_i$ are white noises with zero means and unit variances, $\mathbf{f}_i$ is the self-propulsion force acting on bath particle i with time correlation function $\langle \mathbf{f}_i(t)\mathbf{f}_j(t') \rangle = \frac{D_b}{\mu_b^2 \tau_b} \delta_{ij} e^{-|t-t'|/\tau_b}\mathbf{I}$, where $\mathbf{I}$ is the unit matrix , τ_b is the self-propulsion correlation time and D_b serves as the amplitude of such force, with the same dimension as diffusivity. We consider the situation that all potentials (U and V) are square integrable, meaning that they have well defined and limited Fourier transforms: $U_k = \int U(\mathbf{r})\mathrm{e}^{\mathrm{i}\mathbf{k}\cdot\mathbf{r}}\mathrm{d}\mathbf{r}$, $V_k = \int V(\mathbf{r})\mathrm{e}^{\mathrm{i}\mathbf{k}\cdot\mathbf{r}}\mathrm{d}\mathbf{r}$.

Inspired by the idea of Dean's studies [72, 73], we derive a self-consistent equation for the density profile of bath particles $\rho(\mathbf{r}, t) = \sum_{j=1}^{N} \delta(\mathbf{r} - \mathbf{r}_j(t))$ (See details in Appendix A in Supplementary information),

$$\begin{aligned}\frac{\partial}{\partial t}\rho(\mathbf{r}, t) =& \mu_b \nabla \cdot \left\{\rho(\mathbf{r}, t)\left[\int \rho(\mathbf{r}', t)\nabla V(|\mathbf{r} - \mathbf{r}'|)\mathrm{d}\mathbf{r}'\right.\right.\\ &\left.\left. + \nabla U(|\mathbf{r} - \mathbf{x}|)\right]\right\} + \mu_b T \nabla^2 \rho(\mathbf{r}, t) + \nabla \cdot \left\{\sqrt{\rho(\mathbf{r}, t)}\left[\boldsymbol{\xi}^T(\mathbf{r}, t) + \boldsymbol{\xi}^A(\mathbf{r}, t)\right]\right\}, \end{aligned} \tag{2}$$

where the noise terms $\boldsymbol{\xi}^{\{T,A\}}$ has correlation functions $\langle \boldsymbol{\xi}^T(\mathbf{r}, t)\boldsymbol{\xi}^T(\mathbf{r}', t')\rangle = 2\mu_b T \delta(\mathbf{r}-\mathbf{r}')\delta(t-t')\mathbf{I}$, $\langle \boldsymbol{\xi}^A(\mathbf{r}, t)\boldsymbol{\xi}^A(\mathbf{r}', t')\rangle = \frac{D_b}{\tau_b}\mathrm{e}^{-|t-t'|/\tau_b}\delta(\mathbf{r}-\mathbf{r}')\mathbf{I}$. In the Fourier space ($\delta\rho_k(t) = \int \mathrm{e}^{\mathrm{i}\mathbf{r}\cdot\mathbf{k}}(\rho(\mathbf{r}, t) - \rho_0)\mathrm{d}\mathbf{k}$), Eq. (2) has a formal solution,

$$\delta\rho_k(t) = \int_{-\infty}^{t} \mathrm{e}^{-(t-s)G_k}\Big\{ -\mu_b k^2 \rho_0 U_k \mathrm{e}^{\mathrm{i}\mathbf{k}\cdot\mathbf{x}_s} + \sqrt{\rho_0}\mathrm{i}\mathbf{k} \cdot \left[\tilde{\boldsymbol{\xi}}_k^T(s) + \tilde{\boldsymbol{\xi}}_k^A(s)\right]\Big\}\mathrm{d}s, \tag{3}$$

wherein $G_k = \mu_b k^2(T + \rho_0 V_k)$ can be considered as a characteristic frequency (a typical illustration of this term is shown in Figure S1A). Noise terms $\tilde{\boldsymbol{\xi}}_k^{\{T,A\}}(t)$ are the Fourier transform of $\boldsymbol{\xi}^{\{T,A\}}$, respectively, with correlation functions

$$\left\langle \tilde{\boldsymbol{\xi}}_k^T(t)\tilde{\boldsymbol{\xi}}_{k'}^T(t')\right\rangle = 2\mu_b T(2\pi)^3\delta(\mathbf{k} + \mathbf{k}')\delta(t - t')\mathbf{I}, \tag{4a}$$

$$\left\langle \tilde{\boldsymbol{\xi}}_k^A(t)\tilde{\boldsymbol{\xi}}_{k'}^A(t')\right\rangle = \frac{D_b}{\tau_b}(2\pi)^3\delta(\mathbf{k} + \mathbf{k}')\mathrm{e}^{-|t-t'|/\tau_b}\mathbf{I}, \tag{4b}$$

wherein $\langle\cdots\rangle$ means the average over noises.

Generalized Langevin equation

To achieve an effective equation of motion of the tracer which does not contain any bath particle variables, one can use an identity $\nabla_x \sum_{i=1}^{N} U(|\mathbf{r}_i - \mathbf{x}|) = -\frac{1}{(2\pi)^3}\int \mathrm{i}\mathbf{k}\mathrm{e}^{-\mathrm{i}\mathbf{k}\cdot\mathbf{x}}\rho_k U_k \mathrm{d}^3\mathbf{k}$, then has a GLE for $\mathbf{x}$,

$$\begin{aligned}\dot{\mathbf{x}}(t) =& -\mu_t \nabla_x U_{\mathrm{ext}}(\mathbf{x}) + \mu_t \frac{1}{(2\pi)^3}\int \mathrm{i}\mathbf{k}\mathrm{e}^{-\mathrm{i}\mathbf{k}\cdot\mathbf{x}(t)}\delta\rho_k U_k \mathrm{d}^3\mathbf{k} + \sqrt{2\mu_t T}\boldsymbol{\xi}_t\\ =& -\mu_t \nabla_x U_{\mathrm{ext}}(\mathbf{x}) - \int_{-\infty}^{t} \mathbf{K}(s, t)\mathrm{d}s + \boldsymbol{\eta}_T(t) + \boldsymbol{\eta}_A(t)\sqrt{2\mu_t T}\boldsymbol{\xi}_t,\end{aligned} \tag{5}$$

where the memory kernel

$$\begin{aligned}\mathbf{K}(s, t) =& \frac{\mu_t\mu_b\rho_0}{(2\pi)^3}\int \mathrm{i}k^2\mathbf{k}U_k^2\mathrm{e}^{-(t-s)G_k}\mathrm{e}^{-\mathrm{i}\mathbf{k}\cdot(\mathbf{x}(t)-\mathbf{x}(s))}\mathrm{d}^3\mathbf{k}\\ =& \frac{\mu_t\mu_b\rho_0}{(2\pi)^3}\int \mathrm{Im}[\mathrm{e}^{\mathrm{i}\mathbf{k}\cdot(\mathbf{x}(t)-\mathbf{x}(s))}]\mathbf{k}k^2U_k^2\mathrm{e}^{-(t-s)G_k}\mathrm{d}^3\mathbf{k},\end{aligned} \tag{6}$$

and the colored noise terms,

$$\boldsymbol{\eta}_T(t) = -\mu_t\frac{1}{(2\pi)^3}\int \mathbf{k}\mathrm{e}^{-\mathrm{i}\mathbf{k}\cdot\mathbf{x}_t}\sqrt{\rho_0}U_k\int_{-\infty}^{t}\mathrm{e}^{-(t-s)G_k}\mathbf{k}\cdot\tilde{\boldsymbol{\xi}}_k^T(s)\mathrm{d}s\mathrm{d}^3\mathbf{k}, \tag{7}$$

$$\boldsymbol{\eta}_A(t) = -\mu_t\frac{1}{(2\pi)^3}\int \mathbf{k}\mathrm{e}^{-\mathrm{i}\mathbf{k}\cdot\mathbf{x}_t}\sqrt{\rho_0}U_k\int_{-\infty}^{t}\mathrm{e}^{-(t-s)G_k}\mathbf{k}\cdot\tilde{\boldsymbol{\xi}}_k^A(s)\mathrm{d}s\mathrm{d}^3\mathbf{k}, \tag{8}$$

and their correlations are

$$\mathbf{G}_T(t,t') = \langle \boldsymbol{\eta}_T(t)\boldsymbol{\eta}_T(t')\rangle = \frac{\mu_t^2\rho_0\mu_b T}{(2\pi)^3}\int \mathrm{e}^{-\mathrm{i}\mathbf{k}\cdot(\mathbf{x}_t-\mathbf{x}_{t'})}\mathbf{k}\mathbf{k}k^2U_k^2\frac{\mathrm{e}^{-|t-t'|G_k}}{G_k}\mathrm{d}^3\mathbf{k}, \tag{9}$$

$$\mathbf{G}_A(t,t') = \langle \boldsymbol{\eta}_A(t)\boldsymbol{\eta}_A(t')\rangle = \frac{\mu_t^2\rho_0 D_b}{(2\pi)^3}\int \mathrm{e}^{-\mathrm{i}\mathbf{k}\cdot(\mathbf{x}_t-\mathbf{x}_{t'})}\mathbf{k}\mathbf{k}k^2U_k^2\frac{\tau_b\mathrm{e}^{-|t-t'|/\tau_b}-(\mathrm{e}^{-|t-t'|G_k}/G_k)}{[(\tau_b G_k)^2-1]}\mathrm{d}^3\mathbf{k}. \tag{10}$$

Path integral and effective diffusion

To calculate the transport coefficients, one needs to calculate several correlation functions first. Considering the coupling between the tracer position and the colored noises $\boldsymbol{\eta}_{A,T}$, we propose a path integral method to calculate them.

We consider a path of the tracer in the time interval $[t_i, t_f]$. The partition function of such trajectory can be written as

$$Z = \int\prod_t \delta\Big\{\dot{\mathbf{x}} + \mu_t\nabla U_{\mathrm{ext}} + \int_{-\infty}^{t}\mathbf{K}(s,t)\mathrm{d}s - \boldsymbol{\eta}_A - \boldsymbol{\eta}_T - \sqrt{2\mu_t T}\boldsymbol{\xi}_t\Big\}P[\boldsymbol{\xi}_t]P[\boldsymbol{\eta}_T]P[\boldsymbol{\eta}_A]\mathcal{D}\mathbf{x}\mathcal{D}\boldsymbol{\xi}_t\mathcal{D}\boldsymbol{\eta}_A\mathcal{D}\boldsymbol{\eta}_T. \tag{11}$$

Using the identity of delta function, $\delta(x) = \frac{1}{(2\pi)}\int \mathrm{e}^{\mathrm{i}px}\mathrm{d}p$, we also have

$$Z = \int \mathrm{e}^{\mathrm{i}\int\mathbf{p}\cdot\left\{\dot{\mathbf{x}}+\mu_t\nabla U_{\mathrm{ext}}+\int_{-\infty}^{t}\mathbf{K}(s,t)\mathrm{d}s-\boldsymbol{\eta}_A-\boldsymbol{\eta}_T-\sqrt{2\mu_t T}\boldsymbol{\xi}_t\right\}\mathrm{d}t}P[\boldsymbol{\xi}_t]P[\boldsymbol{\eta}_T]P[\boldsymbol{\eta}_A]\mathcal{D}\mathbf{x}\mathcal{D}\mathbf{p}\mathcal{D}\boldsymbol{\xi}_t\mathcal{D}\boldsymbol{\eta}_A\mathcal{D}\boldsymbol{\eta}_T, \tag{12}$$

where $\mathbf{p}$ is an auxiliary real vector field. Next, utilizing $\langle \mathrm{e}^{au}\rangle = \mathrm{e}^{\frac{1}{2}a^2\langle u^2\rangle}$ for a Gaussian random variable u with zero mean, we have the partition function as a function of the action,

$$Z = \int \mathrm{e}^{-S(\mathbf{x},\mathbf{p})}\mathcal{D}\mathbf{x}\mathcal{D}\mathbf{p}, \quad S(\mathbf{x},\mathbf{p}) = S_0(\mathbf{x},\mathbf{p}) + S_{\mathrm{int}}(\mathbf{x},\mathbf{p}), \tag{13}$$

where

$$S_0 = -\mathrm{i}\int \mathbf{p}(t)\cdot[\dot{\mathbf{x}}(t) + \mu_t\nabla_x U_{\mathrm{ext}}]\,\mathrm{d}t + \mu_t T\int |\mathbf{p}(t)|^2\mathrm{d}t, \tag{14}$$

for a free particle and

$$S_{\mathrm{int}} = -\mathrm{i}\int \mathbf{p}(t)\cdot\left[\int_{-\infty}^{t}\mathbf{K}(s,t)\mathrm{d}s\right]\mathrm{d}t + \frac{1}{2}\iint \mathbf{p}(t)\cdot[\mathbf{G}_T(t,s)+\mathbf{G}_A(t,s)]\cdot\mathbf{p}(s)\mathrm{d}t\mathrm{d}s \tag{15}$$

counts for the tracer-bath interaction. Herein, we have assumed that $\boldsymbol{\eta}_{A,T}$ are both Gaussian, and their deviations from the Gaussian distribution are only weakly present in regions far from the mean. Since this approximation primarily reflects the properties of the second moments, it is reasonable in this context. In addition, since we have used the perturbative expansion, the interaction between tracer and bath particles should be weak. Therefore, we choose soft harmonic potentials as the inter-particle potentials. The perturbation also demands that the activity is not very large, which constitutes a condition for the application of our theoretical framework.

After introducing the partition function over the trajectory, the average over any operator A as function of $\mathbf{x}(t),\ t\in[t_i,t_j]$ can be defined as

$$\langle A\rangle = \frac{\int A\mathrm{e}^{-(S_0+S_{\mathrm{int}})}\mathcal{D}\mathbf{x}\mathcal{D}\mathbf{p}}{Z} = \frac{\langle A\mathrm{e}^{-S_{\mathrm{int}}}\rangle_0}{\langle \mathrm{e}^{-S_{\mathrm{int}}}\rangle_0}, \tag{16}$$

where $\langle \cdots \rangle_0 = Z_0^{-1} \int (\cdots) \mathrm{e}^{-S_0} \mathcal{D}\mathbf{x}\mathcal{D}\mathbf{p}$ corresponds to a tracer particle only affected by external potential, not any particle bath. So far, the $\mathrm{e}^{-S_{\mathrm{int}}}$ term is still too complicated to handle. A common treatment is the linear truncation when S_{int} is weak. Herein, we treat the tracer-bath interaction U as a small perturbative quantity by assigning $U(r) = \sqrt{\epsilon} u(r)$, where ϵ is a dimensionless factor that scales the interacting strength, and can be used to the following perturbative expansion. The memory kernel $\mathbf{k}$ and correlators $G_{A,T}(t)$ are order 1 of ϵ. Therefore, Eq. (16) can be expand as

$$\langle A \rangle = \langle A \rangle_0 - \langle A S_{\mathrm{int}} \rangle_0 + \langle A \rangle_0 \langle S_{\mathrm{int}} \rangle_0 + O(\epsilon^2). \tag{17}$$

For studying the diffusion problem, we only need to consider the free particle situation, $U_{\mathrm{ext}} = 0$. According to the symmetry, we have $\left\langle \mathbf{p}(t) \mathrm{e}^{-\mathrm{i}\mathbf{k}\cdot[\mathbf{x}(t)-\mathbf{x}(s)]} \right\rangle_0 = -\mathrm{i} \langle \mathbf{p}(t)[\mathbf{x}(t) - \mathbf{x}(s)] \rangle_0 \cdot \mathbf{k} \mathrm{e}^{-k^2 \mu_t T(t-s)} = 0$. Similarly, we also have

$$\langle \mathbf{p}(t) \cdot \mathbf{G}_{A,T}(t,s) \cdot \mathbf{p}(t) \rangle_0 \propto \left\{ \left\langle |\mathbf{p}(t)|^2 \right\rangle_0 - (\mathbf{k} \cdot \langle (\mathbf{x}(t) - \mathbf{x}(s)) \mathbf{p}(t) \rangle_0)^2 \right\} \mathrm{e}^{-k^2 \mu_t T(t-s)} = 0. \tag{18}$$

Therefore,

$$\langle S_{\mathrm{int}} \rangle_0 = 0. \tag{19}$$

The next step is to calculate the mean square displacement (MSD), i.e., to calculate $\left\langle [\mathbf{x}(t_f) - \mathbf{x}(t_i)]^2 \right\rangle$ for a long time interval $t_f - t_i$. Then, the effective diffusion coefficient can be given as

$$D_{\mathrm{eff}} = \lim_{(t_f - t_i) \to \infty} \frac{1}{2d(t_f - t_i)} \left\langle [\mathbf{x}(t_f) - \mathbf{x}(t_i)]^2 \right\rangle, \tag{20}$$

where d is the dimension of the system. According to Eq. (17), the key step of calculating the MSD is handling $\left\langle [\mathbf{x}(t_f) - \mathbf{x}(t_i)]^2 S_{\mathrm{int}} \right\rangle_0$, i.e., calculating the following two correlation functions, one is

$$\begin{aligned} &\left\langle [\mathbf{x}(t_f) - \mathbf{x}(t_i)]^2 \mathbf{p}(t) \mathrm{e}^{-\mathrm{i}\mathbf{k}\cdot[\mathbf{x}(t)-\mathbf{x}(s)]} \right\rangle_0 \\ =& -2\mathrm{i}\mathbf{k} \cdot \left\langle [\mathbf{x}(t) - \mathbf{x}(s)][\mathbf{x}(t_f) - \mathbf{x}(t_i)] \right\rangle_0 \left\langle [\mathbf{x}(t_f) - \mathbf{x}(t_i)] \mathbf{p}(t) \right\rangle_0 \mathrm{e}^{-k^2 \mu_t T(t-s)} \\ =& 4\mathbf{k} \mu_t T L([t_i, t_f] \cap [s, t]) \chi_{[t_i, t_f)}(t) \mathrm{e}^{-k^2 \mu_t T(t-s)} \\ =& 4\mathbf{k} \mu_t T [t - \max(t_i, s)] \chi_{[t_i, t_f)}(t) \mathrm{e}^{-k^2 \mu_t T(t-s)}, \end{aligned} \tag{21}$$

and the other is

$$\begin{aligned} &\left\langle [\mathbf{x}(t_f) - \mathbf{x}(t_i)]^2 \mathbf{p}(t) \mathbf{p}(s) \mathrm{e}^{-\mathrm{i}\mathbf{k}\cdot[\mathbf{x}(t)-\mathbf{x}(s)]} \right\rangle_0 \\ =& \left\{ 4\mu_t T [t - \max(s, t_i)] \mathbf{k}\mathbf{k} - 2\chi_{[t_i, t_f)}(s) \mathbf{1} \right\} \mathrm{e}^{-k^2 \mu_t T(t-s)} \chi_{[t_i, t_f)}(t), \end{aligned} \tag{22}$$

for $t > s$ (the omitted mathematical details can be found in Appendix B in Supplementary information). After the calculation in Eq. (S9) (Supplementary information), we get

$$\begin{aligned} \left\langle [\mathbf{x}(t_f) - \mathbf{x}(t_i)]^2 S_{\mathrm{int}} \right\rangle_0 =& 2\mu_t T (t_f - t_i) \frac{\mu_t \mu_b \rho_0}{(2\pi)^3} \int \frac{k^4 U_k^2}{G_k (k^2 \mu_t T + G_k)} \mathrm{d}^3\mathbf{k} \\ &+ \frac{\mu_t^2 \rho_0 D_b}{(2\pi)^3} (t_f - t_i) \int \frac{2k^4 U_k^2}{(\tau_b G_k)^2 - 1} \left\{ \frac{\tau_b \mu_t T k^2 - 1}{(\mu_t T k^2 + \tau_b^{-1})^2} - \frac{(\mu_t T k^2 / G_k) - 1}{(\mu_t T k^2 + G_k)^2} \right\} \mathrm{d}^3\mathbf{k} \\ &+ o(t_f - t_i), \end{aligned} \tag{23}$$

where $G_k = \mu_b k^2(T + \rho_0 V_k)$ reflects the bath properties including background temperature T, number density ρ_0 and interactions between bath particles. At last, taking the long-time limit of $t_f - t_i$, the $o(t_f - t_i)$ term can be neglected, the effective diffusion coefficient of a tracer in an active bath is obtained

$$D_{\mathrm{eff}} = \mu_t T \left\{ 1 - \int_0^\infty g_T(k)\mathrm{d}k + \int_0^\infty g_A(k)\mathrm{d}k \right\}, \tag{24a}$$

to the linear order, wherein

$$g_T(k) = \frac{\mu_t \mu_b \rho_0}{6\pi^2} \frac{k^6 U_k^2}{G_k(k^2\mu_t T + G_k)}, \tag{24b}$$

$$g_A(k) = \frac{\mu_t \rho_0 D_b/T}{6\pi^2} \frac{k^6 U_k^2}{(\tau_b G_k)^2 - 1} \left[\frac{\mu_t T k^2/G_k - 1}{(\mu_t T k^2 + G_k)^2} - \frac{\tau_b \mu_t T k^2 - 1}{(\mu_t T k^2 + \tau_b^{-1})^2} \right]. \tag{24c}$$

This is the main result of the present work. In this equation, "1" in the brace of Eq. (24a) denotes the bare diffusion of a free tracer particle. The second term in the brace denotes the "passive part" of the tracer-bath interaction which is always a negative contribution to effective diffusion and recovers the results in Ref. [70]. In the absence of activity, the FDT holds since the effective mobility of the tracer satisfies $\mu_{\mathrm{eff}} = D_{\mathrm{eff}}/T$ [70], wherein they have obtained an effective mobility coefficient $\mu_{\mathrm{eff}} = \mu_t(1 - \int_0^\infty g_T(k)\mathrm{d}k)$ (expressed with notations of the present work for convenience). The third term is a pure "active" contribution on the diffusion, which is a positive contribution and explicitly gives the nontrivial dependence of D_{eff} on the bath parameters, ρ_0, D_b, τ_b and interactions $U(r)$ and $V(r)$. For this linear truncation, D_{eff} is a linear function of D_b. However, the dependence of τ_b and ρ_0 (which is also contained in G_k) is illegible, which require numerical calculations to determine (see Section "Simulation results"). Further mathematical analysis of this expression is shown in Appendix C in Supplementary information.

SIMULATION RESULTS

In this section, we show numerical calculations of Eq. (24a) with the persistent time of active force τ_b and the number density of bath particles ρ, at small activity D_b region. Then, by comparing these results with computer simulations, the validity and applicability of the theory can be verified.

In the present work, we choose $V(r)$ and $U(r)$ as both harmonic potentials, $V(r) = \frac{\kappa_b}{2}(r - \sigma_{bb})^2$ for $r < \sigma_{bb}$, and $U(r) = \frac{\kappa_t}{2}(r - \sigma_{tb})^2$ for $r < \sigma_{tb}$. We set σ_{bb} as the unit of length, $\kappa_b \sigma_{bb}^2$ as the unit of energy, and $1/(\mu_b \kappa_b)$ as the unit of time. The common parameters are set as: $\sigma_{tb} = 2.0$, $\kappa_t = 1.0$, $\mu_t = 0.333$, $T = 1.0$. The other parameters are set as variables which are explicitly given in the following figures. In computer simulations, we construct a three-dimensional system with periodic boundary containing (1+4095) particles. The diffusion coefficient is calculated through a long-time simulation ($\sim 10^8$ steps with 10^{-3} as the time step) and averaged over 20 samples with random initial configurations.

Firstly, we focus on the contribution of bath number density ρ on D_{eff}, shown in Figure 2. In Figures 2 and 3, dots and corresponding error bars are the direct simulations, and lines are numerical calculation of Eq. (24a). In general, D_{eff} shows a diverse dependence on ρ. For small active force amplitude D_b, D_{eff} decreases with ρ as the tracer's behavior in a passive particle bath. For large activity situation, D_{eff} shows the opposite behavior. Consequently, one may expect that there is a moderate activity region that D_{eff} has a non-monotonic dependence on ρ.

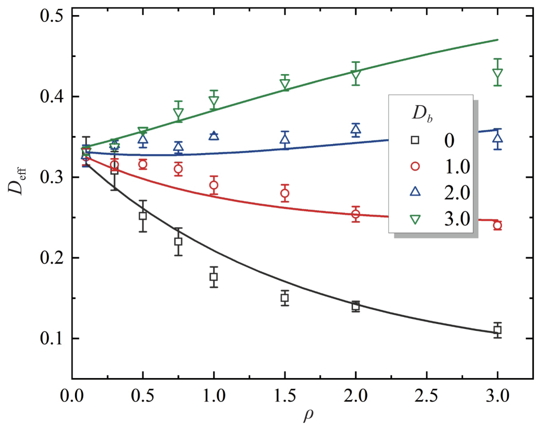

Figure 2 The dependence of the effective diffusion on the number density of active bath particle ρ. Dots and corresponding error bars are simulation results of $D_{\rm eff}$. Solid lines are the numerical calculations of $D_{\rm eff}$. Both results show that, with the increase of activity D_b, effective diffusion $D_{\rm eff}$ gradually changes from monotonic decrease to monotonic increase with the number density of bath particle ρ, including a non-monotonic interval around $D_b = 2.0$. Herein, τ_b is set as 0.1.

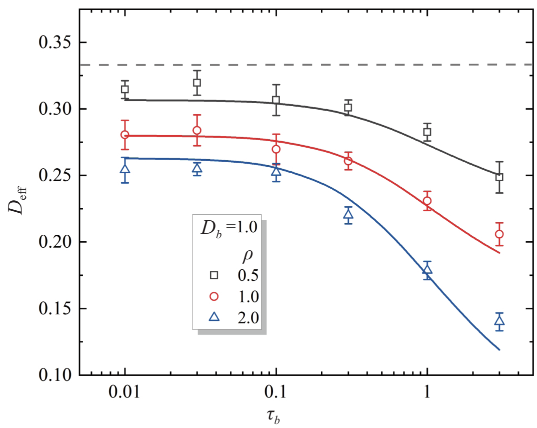

Figure 3 The dependence of the effective diffusion on the active force persistent time τ_b. Dots and corresponding error bars are simulation results of $D_{\rm eff}$. Solid lines are the numerical calculations of $D_{\rm eff}$. Both show that $D_{\rm eff}$ monotonically decreases with the persistent time τ_b. The horizontal dash line denotes the bare diffusion coefficient of the tracer particle.

We then investigate the dependence of $D_{\rm eff}$ on persistent time τ_b. According to Eq. (24a), $D_{\rm eff}$ decreases with τ_b since both $(G_k\tau_b)^2 - 1$ and $\frac{\tau_b\mu_t Tk^2-1}{(\mu_t Tk^2+\tau_b^{-1})^2}$ increase with τ_b monotonically. This prediction has been confirmed in simulations, as shown in Figure 3. Physically, when the persistent time of the active force tends to zero, the active OU particle can be reduced to an ordinary Brownian particle under a higher temperature. If the activity amplitude D_b is constant, the longer τ_b means a larger deviation of equilibrium. Based on the results here, we might conclude that an active OU particle bath that stays closer to equilibrium, is more conducive to the tracer diffusion, when the activity amplitude is given.

CONCLUSION

This study aims to shed light on the intricacies of tracer diffusion in an active particle bath. By employing the generalized Dean's equation, incorporating the path integral method, and utilizing computer simulations, we characterize the impact of self-propulsion on the diffusion behavior of a passive tracer particle. In summary, the effective diffusion decreases with persistent time τ_b, and exhibits a variety of dependencies on bath density, depending on D_b. The obtained insights expand our understanding of collective dynamics and transport phenomena in non-equilibrium systems, with potential applications in diverse scientific disciplines. For further studies, an extension of the active bath situation is straightforward since it has been confirmed to calculate the mobility of a tracer in particle bath [70, 71]. Additionally, after the effective mobility is achieved, the fluctuation-dissipation theorem can be further investigated to determine its validity or deviations with respect to the activity parameters.

Funding

This work was supported by the Strategic Priority Research Program of the Chinese Academy of Sciences (XDB0450402), and the National Natural Science Foundation of China (32090040 and 22373090).

Author contributions

H.Z. directed the project. F.M. derived the theory, wrote codes, and wrote the manuscript. All authors commented on the manuscript.

Conflict of interest

The authors declare no conflict of interest.

Supplementary information

The supporting information is available online at https://doi.org/10.1360/nso/20220069. The supporting materials are published as submitted, without typesetting or editing. The responsibility for scientific accuracy and content remains entirely with the authors.

References

1 Czirók A, Vicsek T. Collective behavior of interacting self-propelled particles. *Phys A-Stat Mech Appl* 2000; **281**: 17–29.

2 Marchetti MC, Joanny JF, Ramaswamy S, *et al*. Hydrodynamics of soft active matter. *Rev Mod Phys* 2013; **85**: 1143–1189.

3 Elgeti J, Winkler RG, Gompper G. Physics of microswimmers-single particle motion and collective behavior: A review. *Rep Prog Phys* 2015; **78**: 056601.

4 Bechinger C, Di Leonardo R, Löwen H, *et al*. Active particles in complex and crowded environments. *Rev Mod Phys* 2016; **88**: 045006.

5 Wu XL, Libchaber A. Particle diffusion in a quasi-two-dimensional bacterial bath. *Phys Rev Lett* 2000; **84**: 3017–3020.

6 Dombrowski C, Cisneros L, Chatkaew S, *et al*. Self-concentration and large-scale coherence in bacterial dynamics. *Phys Rev Lett* 2004; **93**: 098103.

7 Peng Y, Lai L, Tai YS, *et al*. Diffusion of ellipsoids in bacterial suspensions. *Phys Rev Lett* 2016; **116**: 068303.

8 Liu P, Ye S, Ye F, *et al*. Constraint dependence of active depletion forces on passive particles. *Phys Rev Lett* 2020; **124**: 158001.

9 Ye S, Liu P, Ye F, *et al*. Active noise experienced by a passive particle trapped in an active bath. *Soft Matter* 2020; **16**: 4655–4660.

10 Kanazawa K, Sano TG, Cairoli A, *et al*. Loopy Lévy flights enhance tracer diffusion in active suspensions. *Nature* 2020; **579**: 364–367.

11 Shea J, Jung G, Schmid F. Passive probe particle in an active bath: Can we tell it is out of equilibrium? *Soft Matter* 2022;

18: 6965–6973.
12 Cheng K, Liu P, Yang M, *et al*. Experimental investigation of active noise on a rotor in an active granular bath. *Soft Matter* 2022; **18**: 2541–2548.
13 Kurihara T, Aridome M, Ayade H, *et al*. Non-Gaussian limit fluctuations in active swimmer suspensions. *Phys Rev E* 2017; **95**: 030601.
14 Ariga T, Tomishige M, Mizuno D. Nonequilibrium energetics of single molecule motor, kinesin-1. *Biophys J* 2018; **114**: 509a.
15 Ariga T, Tomishige M, Mizuno D. Experimental and theoretical energetics of walking molecular motors under fluctuating environments. *Biophys Rev* 2020; **12**: 503–510.
16 Ning L, Lou X, Ma Q, *et al*. Hydrodynamics-induced long-range attraction between plates in bacterial suspensions. *Phys Rev Lett* 2023; **131**: 158301.
17 Liebchen B, Löwen H. Synthetic chemotaxis and collective behavior in active matter. *Acc Chem Res* 2018; **51**: 2982–2990.
18 Zhao H, Košmrlj A, Datta SS. Chemotactic motility-induced phase separation. *Phys Rev Lett* 2023; **131**: 118301.
19 Suma A, Cugliandolo LF, Gonnella G. Tracer motion in an active dumbbell fluid. *J Stat Mech* 2016; **5**: 054029.
20 Krishnamurthy S, Ghosh S, Chatterji D, *et al*. A micrometre-sized heat engine operating between bacterial reservoirs. *Nat Phys* 2016; **12**: 1134–1138.
21 Martínez IA, Roldán É, Dinis L, *et al*. Colloidal heat engines: A review. *Soft Matter* 2017; **13**: 22–36.
22 Burkholder EW, Brady JF. Tracer diffusion in active suspensions. *Phys Rev E* 2017; **95**: 052605.
23 Saha A, Marathe R. Stochastic work extraction in a colloidal heat engine in the presence of colored noise. *J Stat Mech* 2019; **9**: 094012.
24 Lee JS, Park JM, Park H. Brownian heat engine with active reservoirs. *Phys Rev E* 2020; **102**: 032116.
25 Goswami K. Work fluctuations in a generalized Gaussian active bath. *Phys A-Stat Mech Appl* 2021; **566**: 125609.
26 Seyforth H, Gomez M, Rogers WB, *et al*. Nonequilibrium fluctuations and nonlinear response of an active bath. *Phys Rev Res* 2022; **4**: 023043.
27 Tociu L, Rassolov G, Fodor É, *et al*. Mean-field theory for the structure of strongly interacting active liquids. *J Chem Phys* 2022; **157**: 014902.
28 Datta A, Pietzonka P, Barato AC. Second law for active heat engines. *Phys Rev X* 2022; **12**: 031034.
29 Feng M, Hou Z. Unraveling on kinesin acceleration in intracellular environments: A theory for active bath. *Phys Rev Res* 2023; **5**: 013206.
30 Das B, Paul S, Manikandan SK, *et al*. Enhanced directionality of active processes in a viscoelastic bath. *New J Phys* 2023; **25**: 093051.
31 Saha TK, Ehrich J, Gavrilov M, *et al*. Information engine in a nonequilibrium bath. *Phys Rev Lett* 2023; **131**: 057101.
32 Semeraro M, Gonnella G, Suma A, *et al*. Work fluctuations for a harmonically confined active ornstein-uhlenbeck particle. *Phys Rev Lett* 2023; **131**: 158302.
33 Kim MJ, Breuer KS. Enhanced diffusion due to motile bacteria. *Phys Fluids* 2004; **16**: L78–L81.
34 Maggi C, Paoluzzi M, Pellicciotta N, *et al*. Generalized energy equipartition in harmonic oscillators driven by active baths. *Phys Rev Lett* 2014; **113**: 238303.
35 Maes C. On the second fluctuation-dissipation theorem for nonequilibrium baths. *J Stat Phys* 2014; **154**: 705–722.
36 Maggi C, Marconi UMB, Gnan N, *et al*. Multidimensional stationary probability distribution for interacting active particles. *Sci Rep* 2015; **5**: 10742.
37 Maggi C, Paoluzzi M, Angelani L, *et al*. Memory-less response and violation of the fluctuation-dissipation theorem in colloids suspended in an active bath. *Sci Rep* 2017; **7**: 17588.
38 Lagarde A, Dagès N, Nemoto T, *et al*. Colloidal transport in bacteria suspensions: From bacteria collision to anomalous and enhanced diffusion. *Soft Matter* 2020; **16**: 7503–7512.

39 Banerjee T, Jack RL, Cates ME. Tracer dynamics in one dimensional gases of active or passive particles. *J Stat Mech* 2022; **1**: 013209.

40 Vicsek T, Zafeiris A. Collective motion. *Phys Rep* 2012; **517**: 71–140.

41 Sumino Y, Nagai KH, Shitaka Y, *et al*. Large-scale vortex lattice emerging from collectively moving microtubules. *Nature* 2012; **483**: 448–452.

42 Sokolov A, Aranson IS. Physical properties of collective motion in suspensions of bacteria. *Phys Rev Lett* 2012; **109**: 248109.

43 Marchetti MC, Joanny JF, Ramaswamy S, *et al*. Hydrodynamics of soft active matter. *Rev Mod Phys* 2013; **85**: 1143–1189.

44 Liu P, Zhu H, Zeng Y, *et al*. Oscillating collective motion of active rotors in confinement. *Proc Natl Acad Sci USA* 2020; **117**: 11901–11907.

45 Loewe B, Shendruk TN. Passive Janus particles are self-propelled in active nematics. *New J Phys* 2022; **24**: 012001.

46 Su J, Feng M, Du Y, *et al*. Motility-induced phase separation is reentrant. *Commun Phys* 2023; **6**: 58.

47 Hänggi P, Marchesoni F. Artificial brownian motors: Controlling transport on the nanoscale. *Rev Mod Phys* 2009; **81**: 387–442.

48 Cates ME. Diffusive transport without detailed balance in motile bacteria: Does microbiology need statistical physics? *Rep Prog Phys* 2012; **75**: 042601.

49 Koumakis N, Maggi C, Di Leonardo R. Directed transport of active particles over asymmetric energy barriers. *Soft Matter* 2014; **10**: 5695–5701.

50 Mano T, Delfau JB, Iwasawa J, *et al*. Optimal run-and-tumble-based transportation of a Janus particle with active steering. *Proc Natl Acad Sci USA* 2017; **114**: E2580–E2589.

51 Granek O, Kafri Y, Tailleur J. Anomalous transport of tracers in active baths. *Phys Rev Lett* 2022; **129**: 038001.

52 Mallory SA, Valeriani C, Cacciuto A. Curvature-induced activation of a passive tracer in an active bath. *Phys Rev E* 2014; **90**: 032309.

53 Maes C, Steffenoni S. Friction and noise for a probe in a nonequilibrium fluid. *Phys Rev E* 2015; **91**: 022128.

54 Maes C. Fluctuating motion in an active environment. *Phys Rev Lett* 2020; **125**: 208001.

55 Park JT, Paneru G, Kwon C, *et al*. Rapid-prototyping a Brownian particle in an active bath. *Soft Matter* 2020; **16**: 8122–8127.

56 Reichert J, Voigtmann T. Tracer dynamics in crowded active-particle suspensions. *Soft Matter* 2021; **17**: 10492–10504.

57 Solon A, Horowitz JM. On the Einstein relation between mobility and diffusion coefficient in an active bath. *J Phys A-Math Theor* 2022; **55**: 184002.

58 Baiesi M, Maes C, Wynants B. Fluctuations and response of nonequilibrium states. *Phys Rev Lett* 2009; **103**: 010602.

59 Ruben Gomez-Solano J, Petrosyan A, Ciliberto S, *et al*. Fluctuations and response in a non-equilibrium micron-sized system. *J Stat Mech* 2011; **1**: P01008.

60 Maes C, Safaverdi S, Visco P, *et al*. Fluctuation-response relations for nonequilibrium diffusions with memory. *Phys Rev E* 2013; **87**: 022125.

61 Basu U, Maes C. Nonequilibrium response and frenesy. *J Phys-Conf Ser* 2015; **638**: 012001.

62 Maes C. Frenesy: Time-symmetric dynamical activity in nonequilibria. *Phys Rep* 2020; **850**: 1–33.

63 Maes C. Response theory: A trajectory-based approach. *Front Phys* 2020; **8**: 229.

64 Krüger M, Maes C. The modified Langevin description for probes in a nonlinear medium. *J Phys-Condens Matter* 2017; **29**: 064004.

65 Seifert U, Speck T. Fluctuation-dissipation theorem in nonequilibrium steady states. *Europhys Lett* 2010; **89**: 10007.

66 Mehl J, Blickle V, Seifert U, *et al*. Experimental accessibility of generalized fluctuation-dissipation relations for nonequilibrium steady states. *Phys Rev E* 2010; **82**: 032401.

67 Lander B, Seifert U, Speck T. Mobility and diffusion of a tagged particle in a driven colloidal suspension. *EPL* 2010;

92: 58001.

68 Esparza López C, Théry A, Lauga E. A stochastic model for bacteria-driven micro-swimmers. *Soft Matter* 2019; **15**: 2605–2616.

69 Burkholder EW, Brady JF. Fluctuation-dissipation in active matter. *J Chem Phys* 2019; **150**: 184901.

70 Démery V, Dean DS. Perturbative path-integral study of active- and passive-tracer diffusion in fluctuating fields. *Phys Rev E* 2011; **84**: 011148.

71 Démery V, Bénichou O, Jacquin H. Generalized Langevin equations for a driven tracer in dense soft colloids: Construction and applications. *New J Phys* 2014; **16**: 053032.

72 Dean DS. Langevin equation for the density of a system of interacting Langevin processes. *J Phys A-Math Gen* 1996; **29**: L613–L617.

73 Démery V, Dean DS. Drag forces in classical fields. *Phys Rev Lett* 2010; **104**: 080601.